Hindawi Publishing Corporation
EURASIP Journal on Wireless Communications and Networking
Volume 2007, Article ID 57175, 10 pages
doi:10.1155/2007/57175

Research Article

Employing Coordinated Transmit and Receive Beamforming in Clustering Double-Directional Radio Channel

Chen Sun,[1] Makoto Taromaru,[1] and Takashi Ohira[2]

[1] *ATR Wave Engineering Laboratories, 2-2-2 Hikaridai, Keihanna Science City, Kyoto 619-0288, Japan*
[2] *Department of Information and Computer Sciences, Toyohashi University of Technology, 1-1 Hibariga-oka, Toyohashi 441-8580, Japan*

Received 31 October 2006; Accepted 1 August 2007

Recommended by Robert W. Heath Jr.

A novel beamforming (BF) system that employs two switched beam antennas (SBAs) at both ends of the wireless link in an indoor double-directional radio channel (DDRC) is proposed. The distributed directivity gain (DDG) and beam pattern correlation in DDRC are calculated. The channel capacity of the BF system is obtained from an analytical model. Using the channel capacity and outage capacity as performance measures, we show that the DDG of the BF system directly increases the average signal-to-noise ratio (SNR) of the wireless link, thus achieving a direct increase of the ergodic channel capacity. By jointly switching between different pairs of transmit (Tx) and receive (Rx) directional beam patterns towards different wave clusters, the system provides diversity gain to combat against multipath fading, thus reducing the outage probability of the random channel capacity. Furthermore, the performance of the BF system is compared with that of a multiple-input multiple-output (MIMO) system that is set up using linear antenna arrays. Results show that in a low-SNR environment, the BF system outperforms the MIMO system in the same clustering DDRC.

1. INTRODUCTION

Along with the evolution of wireless technologies, broadband Internet access and multimedia services are expected to be available for commercial mobile subscribers. This enthusiasm has created a need for high-data-rate wireless transmission systems. Study on adaptive antenna systems has demonstrated their potential in increasing the spectrum efficiency of a wireless radio channel. The beamforming (BF) ability of the adaptive antennas increases the transmission range, reduces delay spread, and suppresses interference [1–4]. In a multipath rich environment, they provide diversity gain to counteract multipath fading [5, 6]. Installing antenna arrays at both transmitter (Tx) and receiver (Rx) sides builds up a multiple-input multiple-output (MIMO) system [7]. The MIMO system increases the data rate of wireless transmission by sending multiple data streams though multiple Tx and Rx antennas over fading channels [8].

The potential increase in the spectrum efficiency of the MIMO systems has been evaluated under various wireless propagation channel models. Recent investigation on wireless channel model has introduced the concept of double-directional radio channel (DDRC) that incorporates directional information at both Tx and Rx sides of a wireless link [9]. The techniques of extracting directional information at both ends of the wireless link are presented in [10, 11]. In [11] Wallace and Jensen extend the Saleh-Valenzuela's clustering model [12] and the Spencer's model [13] to include both angle-of-arrival (AOA) information and angle-of-departure (AOD) information to describe an indoor DDRC with clustering phenomenon, which is here after referred to as *clustering DDRC*. Incorporating spatial information at both ends of the link, the statistical model provides a better description of a wireless propagation channel, thus allowing a better evaluation of the system performance in a practical situation than other models. The channel capacity that can be achieved by a MIMO system in a clustering DDRC model is evaluated in [11]. The predicted capacities match perfectly with the measured data. This justifies the clustering DDRC model being a better description of a practical wireless propagation channel independently of specific antenna characteristics.

However, the predicted capacity of a MIMO system in a clustering DDRC model is lower than that predicted under

an ideal statistical channel model, which assumes statistically independent fading at antenna array elements [7]. The reason is that the potential capacity of MIMO systems relies on the richness of scattering waves. The clustering phenomenon of impinging waves in the Wallace's model [11] leads to an increase of fading correlation among antenna array elements, thus resulting in a lower-channel capacity.

In addition to the capacity loss of a MIMO system in a clustering channel, the implementation of a MIMO system poses practical problems, such as the power consumption limitation and the size constraints of commercial mobile terminals. A MIMO receiver that is equipped with an antenna array consists of multiple RF channels connected to individual array elements so that spatial processing (such as BF, diversity combining) is carried out at digital stage. The power consumption and fabrication cost of the MIMO system increase with the number of array elements.

To circumvent the afore-mentioned limitations of the MIMO system and to increase the channel capacity of wireless communication in a clustering DDRC, we propose a BF system that employs two switched beam antennas (SBAs) with predefined directional beam patterns at both ends of the wireless link. Knowing that the main energy of the signals is transported spatially through wave clusters [14], the directional beam patterns at both Tx and Rx sides are directed towards the wave clusters. Employing the directional beam pattern in the presence of distributed waves, the distributed directivity gains (DDGs) at both Tx and Rx antennas directly increase the average SNR of the wireless link. By switching between different pairs of Tx and Rx directional beam patterns, the system provides a diversity freedom to further improve the performance.

A potential application of the proposed technique is an ad hoc network. It is a self-configuring network of mobile terminals without a wireless backbone, such as access points [3]. Commercial applications of adaptive antenna technology at these battery-powered mobile terminals (e.g., laptops, PDAs) require adaptive antennas that have low-power consumption and low-fabrication cost. The parasitic array antennas have shown their potential in fulfilling the goal [3]. Therefore, in this paper, the Tx and Rx SBAs are realized by two electronically steerable parasitic array radiator (ESPAR) antennas [15–17]. We do not employ a multibeam antennas as their structures consist of a number of individual RF channel that lead to undesirable high-power consumption and fabrication cost [3].

The rest of the paper is organized as follows. In Section 2, we describe the clustering DDRC model, the SBA and the BF system. In Section 3, we calculate the DDG at both ends of the wireless link. The correlation of different wireless links that are set up with different pairs of transmit and receive beam patterns is obtained. Based on these results, an analytical model of the BF system is built. In Section 4, we calculate the channel capacity of the BF system based on the analytical model and compare the performance of the BF system with a MIMO system in the same clustering DDRC model. Finally, in Section 5, we conclude the paper.

2. SYSTEM MODEL

In order to present the system model of the proposed BF system, we review the clustering DDRC model first. After that, the ESPAR antennas that operate as SBAs in the proposed system are described. Finally, the BF system that employs two ESPAR antennas at both ends of the wireless link in a clustering DDRC is given.

2.1. Clustering DDRC

In [12] Saleh and Valenzuela describe the clustering phenomenon of impinging waves in an indoor multipath channel, that is, the result of scattering and reflection on small objects, rough surface, and so forth, along the paths of wave propagation In [13]Spencer et al. extend Saleh's model according to the measurement results to include spatial information of the clusters and waves within each cluster. The Spencer's model is further extended in [11] to describe a clustering DDRC, which takes into account the spatial information at both Tx and Rx sides.

The spatial channel response (SCR) of a clustering DDRC is written as [11]

$$h(\phi^r,\phi^t) = \frac{1}{\sqrt{LK}}\sum_{l=0}^{L-1}\sum_{k=0}^{K-1}\alpha_{l,k} \times \delta(\phi^r-\Phi_l^r-\omega_{l,k}^r)\delta(\phi^t-\Phi_l^t-\omega_{l,k}^t), \tag{1}$$

where superscripts $(\cdot)^r$ and $(\cdot)^t$ denote, respectively, the Rx and Tx sides of a wireless link. Let ϕ^r and ϕ^t represent the AOA and AOD, respectively. The nominal AOA and AOD of the lth cluster are denoted by Φ_l^r and Φ_l^t, which are uniformly distributed over the azimuthal plane [13]. Here, L is the total number of wave clusters. In the following discussion, we call the waves within each cluster as *rays* and let $\omega_{l,k}^r$ and $\omega_{l,k}^t$ denote, respectively, the AOA and AOD of the kth ray within the lth cluster. Within each wave cluster, there are totally K rays. Furthermore, $\omega_{l,k}^r$ and $\omega_{l,k}^t$ follow a Laplacian distribution centered at Φ_l^r and Φ_l^t, respectively, as

$$f_\omega(\omega_{l,k} \mid \Phi_l) = \frac{1}{\sqrt{2}\sigma}e^{-|\sqrt{2}(\omega_{l,k}-\Phi_l)/\sigma|}, \tag{2}$$

where σ is the angular spread of rays within each cluster. In (1), the amplitude of $\alpha_{l,k}$ associated with the kth ray in the lth cluster is assumed to follow a Rayleigh distribution [11, 13] with the mean power following a double-exponential distribution. That is,

$$E[\alpha_{l,k}^2] = E[\alpha_{0,0}^2]e^{-\Gamma_l/\Gamma}e^{-\Gamma_{l,k}/\gamma}, \tag{3}$$

where $E[\cdot]$ is the expectation operator. $\alpha_{0,0}^2$ is the power decay of the first ray of the first cluster with $E[\alpha_{0,0}^2] = 1$. Γ and γ are the constant decay time of cluster and rays, respectively. Γ_l is the delay of the first arrival ray of the lth cluster and $\Gamma_0 = 0$ nanosecond. It is exponentially distributed and conditioned on Γ_{l-1} as

$$f_\Gamma(\Gamma_l \mid \Gamma_{l-1}) = \Lambda e^{-\Lambda(\Gamma_l-\Gamma_{l-1})}, \quad 0 \le \Gamma_{l-1} < \Gamma_l < \infty. \tag{4}$$

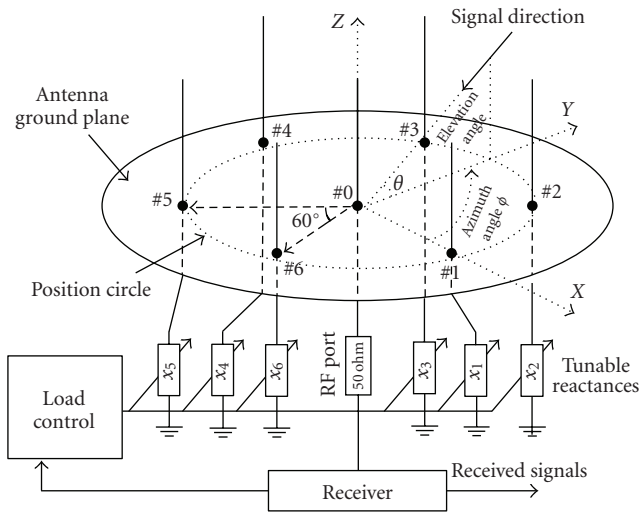

Figure 1: Structure of a 7-element ESPAR antenna. The elements are monopoles with interelement spacing of a quarter wavelength.

The delay of rays $\tau_{l,k}$ within each cluster is also exponentially distributed and conditioned on the previous delay $\tau_{l,k-1}$ as

$$f_\tau(\tau_{l,k} \mid \tau_{l,k-1}) = \lambda e^{-\lambda(\tau_{l,k}-\tau_{l,k-1})}, \quad 0 \le \tau_{l,k-1} < \tau_{l,k} < \infty. \tag{5}$$

Here, Λ and λ are the constant arrival rates of clusters and rays, respectively. The statistics of rays and clusters are assumed being independent [11, 13], that is,

$$f_{\tau,\omega}(\tau_{l,k}, \omega_{l,k} \mid \tau_{l,k-1}) = f_\tau(\tau_{l,k} \mid \tau_{l,k-1}) f_\omega(\omega_{l\cdot k}). \tag{6}$$

In this study, we set $\Gamma = 30$ nanoseconds, $\gamma = 20$ nanoseconds, $1/\Lambda = 30$ nanoseconds, $1/\lambda = 5$ nanoseconds, and $\sigma = 20^\circ$ to represent an indoor or urban microscopic environment as in [12].

2.2. ESPAR antenna

In this paper, two parasitic array antennas named as ESPAR [15, 16] are employed at both ends of the wireless link to produce Tx and Rx directional beam patterns. In this subsection, we briefly explain the operation principle of an ESPAR antenna.

Figure 1 shows the structure of a seven-element ESPAR antenna. There, one active central monopole is surrounded by parasitic elements on a circle of radius of a quarter wavelength on the circular grounded base plate. The central monopole is connected to an RF receiver and each parasitic monopole is loaded with a tunable reactance. Let $s(t)$ be the far-field impinging wave from direction ϕ, the output signal at the RF port is written as

$$y(t) = \mathbf{w}_{\text{ESP}}^T \boldsymbol{\alpha}(\phi) s(t) + n(t), \tag{7}$$

where $\boldsymbol{\alpha}(\phi)$ is the 7-by-1 dimensional steering vector defined based upon the array geometry of the ESPAR antenna. It is written as

$$\boldsymbol{\alpha}(\phi) = [\ \text{A1}\ \ \text{A2}\ \ \text{A3}\ \ \text{A4}\ \ \text{A5}\ \ \text{A6}\ \ \text{A7}\ ]^T, \tag{8}$$

where A1 = 1, A2 = $e^{j(\pi/2)\cos(\phi)}$, A3 = $e^{j(\pi/2)\cos(\phi-\pi/3)}$, A4 = $e^{j(\pi/2)\cos(\phi-2\pi/3)}$, A5 = $e^{j(\pi/2)\cos(\phi-\pi)}$, A6 = $e^{j(\pi/2)\cos(\phi-4\pi/3)}$, A7 = $e^{j(\pi/2)\cos(\phi-5\pi/3)}$, In (7), $n(t)$ denotes an additive white Gaussian noise (AWGN) component. Superscript $(\cdot)^T$ denotes transpose. $\mathbf{w}_{\text{ESP}}$ is written as

$$\mathbf{w}_{\text{ESP}} = z_0 \left(\mathbf{Y}^{-1} + \mathbf{X}\right)^{-1} \mathbf{u}_1, \tag{9}$$

where $\mathbf{Y}$ is a mutual admittance matrix of array elements. The values of entities of $\mathbf{Y}$ are calculated using a method of moment (MoM) Numerical Electromagnetic Code (NEC) simulator [18] and are given in [16]. Matrix $\mathbf{X}$ is a diagonal matrix given by $\text{diag}[z_0, jx_1, \ldots, jx_6]$, where $x_i (i = 1, 2, \ldots, 6)$ $[\Omega]$ is the reactance loaded at the array parasitic elements as shown in Figure 1. The characteristic impedance at the central RF port is $z_0 = 50$ $[\Omega]$. In (9), $\mathbf{u}_1$ is defined as $\text{u}_1 = [\ 1\ \ 0\ \ 0\ \ 0\ \ 0\ \ 0\ \ 0\ ]^T$. From (7), we can see that $\mathbf{w}_{\text{ESP}}$ is equivalent to an array BF weight vector. Here, we write the normalized $\mathbf{w}_{\text{ESP}}$ as

$$\mathbf{w} = \frac{\mathbf{w}_{\text{ESP}}}{\sqrt{\mathbf{w}_{\text{ESP}}^H \mathbf{w}_{\text{ESP}}}}. \tag{10}$$

The normalized azimuthal directional beam pattern for a given weight vector $\mathbf{w}$ is written as

$$g(\phi \mid \mathbf{w}) = \frac{\left|\mathbf{w}^T \boldsymbol{\alpha}(\phi)\right|^2}{(1/2\pi)\int_0^{2\pi} \mathbf{w}^T \boldsymbol{\alpha}(\phi) \boldsymbol{\alpha}^H(\phi) \mathbf{w}^* d\phi}, \tag{11}$$

where superscript $(\cdot)^*$ is the complex-conjugate. In this study we have neglected the effect of load mismatch. For simplicity, we only consider the impinging waves that are copolarized with the array elements in the azimuthal plane. Since $\mathbf{w}$ is dependent on the tunable reactances loaded at those parasitic elements, changing the values of reactance, the beam adjusts the beam pattern of an ESPAR antenna. This model describes the beam pattern control based on tuning the loaded reactances at the parasitic elements. It enables us to examine the system performance at different setting of reactance values. The validity of this model has been proved by experiments and simulation based on (7)–(11) in [16].

In this paper, we use the ESPAR to generate a few predefined directional beam patterns and employ the antenna as an SBA. When the reactance values are set to $(-9\,000\,000)$ $[\Omega]$, the ESPAR antenna forms a directional beam pattern pointing to 0° in the azimuthal plane. The 3D beam pattern that is produced using the NEC simulator is shown in Figure 2. The azimuthal plane of this simulated beam pattern using an NEC simulator is compared with the calculated beam pattern with MATLAB using (11) and the measured beam pattern in Figure 3. Since the three beam patterns match closely, we use (11) to describe a beam pattern that is generated by an ESPAR antenna in the following analysis. By shifting the reactance values, the antenna produces six consecutive beam patterns as shown in Figure 4. The reactance values for those six directional beam patterns are listed in Table 1. In the following analysis, we use $\mathbf{w}_m$, $m = 1, 2, \ldots, 6$, to denote the ESPAR weight vector that is described in (10) for the six directional beam patterns pointing to $(m-1)\times 60^\circ$ in the azimuthal plane. $g(\phi \mid \mathbf{w}_m)$ is the corresponding normalized directional beam pattern as described in (11).

Table 1: Reactance values for different directional beam patterns.

Equivalent weight	Beam azimuthal direction	x_1	x_2	x_3	x_4	x_5	x_6
w_1	0°	−90	0	0	0	0	0
w_2	60°	0	−90	0	0	0	0
w_3	120°	0	0	−90	0	0	0
w_4	180°	0	0	0	−90	0	0
w_5	240°	0	0	0	0	−90	0
w_6	300°	0	0	0	0	0	−90

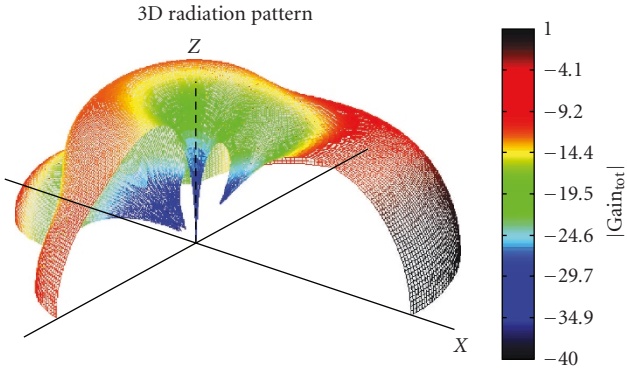

Figure 2: Three-dimensional beam pattern of a 7-element ESPAR antenna that is calculated by NEC simulator. X = [−9 000 000]Ω. The directional beam pattern is pointing to 0° in the azimuthal plane.

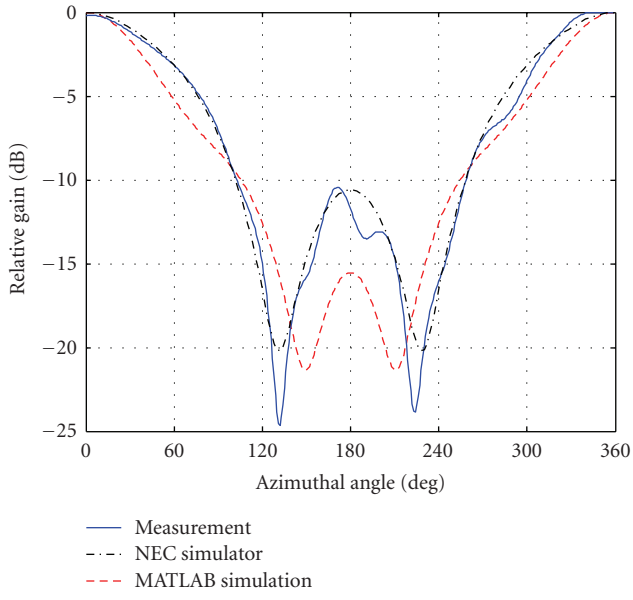

Figure 3: Comparison of the directional beam patterns of measurement and simulation using MATLAB and NEC simulator.

2.3. BF system

Two ESPAR antennas are employed at both ends of the wireless link. When both the Tx and Rx directional beam patterns are steered towards one of the existing clusters, the link is set up. This prerequisites a cluster identification process.

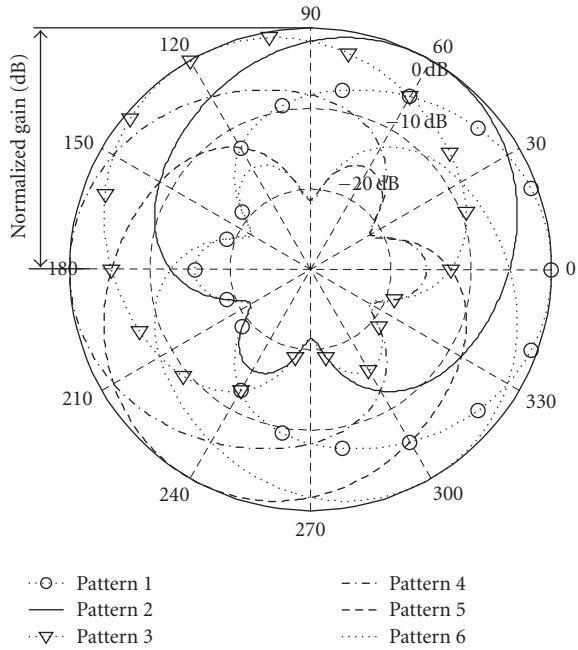

Figure 4: Six consecutive directional beam patterns generated by shifting the reactance values.

In [9, 13, 19], wave clusters are identified in spatial-temporal domain through visual observation. In this paper, we assume that the clusters' spatial information is known at both Tx and Rx sides, and the directional beam patterns at both ends of the link can be steered towards a common wave cluster. As shown in Figure 5, there are two clusters of waves at both the Tx and Rx sides. Both Tx and Rx can choose one out of six predefined directional beam patterns pointing to a common wave cluster.

3. PERFORMANCE EVALUATION

Given the above model, the question that arises is how much capacity this system can provide. In order to calculate the channel capacity, in this section, we examine the directivity gain and the beam pattern correlation in a clustering DDRC model. The channel capacity will be given in Section 4.

3.1. DDG

Firstly, we examine the directivity gain of the beam pattern for the system model. Analyzing the directivity gain in

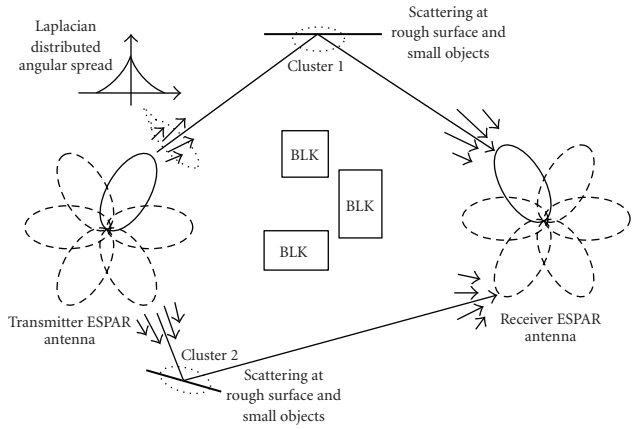

Figure 5: System model of employing directional antennas at both ends of the wireless link in a clustering DDRC.

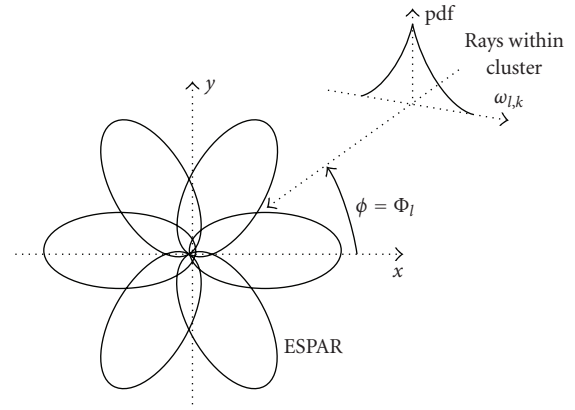

Figure 6: The impinging waves from a cluster with nominal direction Φ_l on directional beam patterns of the ESPAR antenna.

the presence of angular distribution of the impinging waves invokes calculating the DDG [20]. Since we only consider waves in the azimuthal plane, the DDG can be given as

$$D(\Phi, \sigma, \mathbf{w}) = \eta_{\text{ant}} 2\pi \int_0^{2\pi} f_\omega(\phi \mid \Phi) g(\phi \mid \mathbf{w}) d\phi, \tag{12}$$

where $f_\omega(\phi \mid \Phi)$ is the probability density function (pdf) of the angular distribution of impinging waves and $g(\phi \mid \mathbf{w})$ is given in (11). Here, η_{ant} is the antenna efficiency that is assumed to be unity. For simplicity, we omit η_{ant} in the following analysis.

Figure 6 shows the situation when there is one cluster centered at Φ_l. The AOAs of rays within the cluster follow Laplacian distribution as expressed in (2). As stated previously, the ESPAR antenna can produce six consecutive directional beam patterns by shifting the reactance values. Let us now calculate the DDG for the directional beam pattern that points to 0° in the azimuthal plane, that is, we use $\mathbf{w}_1$ in (11), while the nominal direction of the cluster is moving from 0° to 180°. In this case, we can calculate the DDG as

$$D(\Phi, \sigma, \mathbf{w}_1) = \frac{\sqrt{2}\pi \int_0^{2\pi} \left| \mathbf{w}_1^T \boldsymbol{\alpha}(\phi) \right|^2 e^{-|\sqrt{2}(\phi - \Phi)/\sigma|} d\phi}{\sigma \int_0^{2\pi} \mathbf{w}_1^T \boldsymbol{\alpha}(\phi) \boldsymbol{\alpha}^H(\phi) \mathbf{w}_1^* d\phi}. \tag{13}$$

The DDG corresponding to different angular spreads is also shown in Figure 7. For the Laplacian distributed scenarios, using a directional beam pattern pointing to a wave cluster provides a significant DDG. However, the DDG degrades as the center of the cluster moves away from the direction of the beam pattern's maximum gain. Please note that when the waves are uniformly distributed over the azimuthal plane, using a directional beam pattern does not provide any DDG.

The DDG calculated in Figure 7 considers only one cluster of impinging waves. For multiple clusters (e.g., two clusters), we can write the angular distribution according to (2) as

$$f_\omega(\phi \mid \Phi_1, \Phi_2) = \frac{1}{2\sqrt{2}\sigma} \left(e^{-|\sqrt{2}(\phi - \Phi_1)/\sigma_1|} + e^{-|\sqrt{2}(\phi - \Phi_2)/\sigma_2|} \right). \tag{14}$$

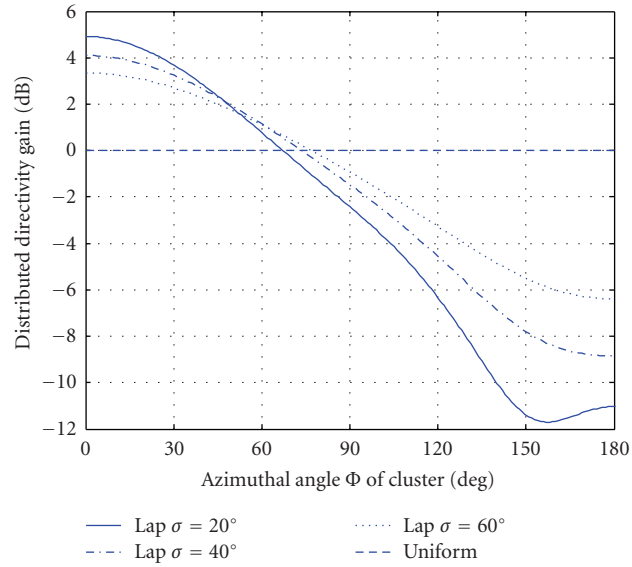

Figure 7: DDG for the directional beam pattern by the ESPAR antennas in different spatially distributed radio channels.

We also follow the assumption in [11, 13] that the angular spreads of all clusters are the same, that is, $\sigma_1 = \sigma_2$. Inserting (14) into (12), we obtain the DDG when there are two clusters as

$$D(\Phi_1, \Phi_2, \sigma, \mathbf{w}_1) = \frac{1}{2} D(\Phi_1, \sigma, \mathbf{w}_1) + \frac{1}{2} D(\Phi_2, \sigma, \mathbf{w}_1). \tag{15}$$

3.2. Link gain

By now, we have calculated the DDG at one (Tx or Rx) side of the wireless link. Because both the Tx and Rx employ directional beam patterns, the joint directivity gain incorporates the directivity gains at both sides of the link. This is in accordance with the concept of DDRC. Given the SRC of a

clustering DDRC in (1) and the beam pattern in (11), the spatial channel model of the BF system is given by

$$h_{\mathrm{BF}} = \sqrt{g(\phi^r \mid \mathbf{w}_m^r)} * h(\phi^r, \phi^t) * \sqrt{g(\phi^t \mid \mathbf{w}_m^t)} = \frac{1}{\sqrt{LK}} \sum_{l=0}^{L-1} \sum_{k=0}^{K-1} \alpha_{l,k} \sqrt{g(\Phi_l^r + \omega_{l,k}^r \mid \mathbf{w}_m^r)} \sqrt{g(\Phi_l^t + \omega_{l,k}^t \mid \mathbf{w}_m^t)}, \tag{16}$$

where $\mathbf{w}_m^r$ and $\mathbf{w}_m^t$ are the BF weight vectors at the Rx side and Tx sides, respectively. Taking the expectation of $|h_{\mathrm{BF}}|^2$ in (16), we obtain the link gain as

$$G = E[h_{\mathrm{BF}} h_{\mathrm{BF}}^H] = \frac{1}{LK} \sum_{l=0}^{L-1} \sum_{k=0}^{K-1} E[\alpha_{l,k} \alpha_{l,k}^*] \times E[g(\Phi_l^r + \omega_{l,k}^r \mid \mathbf{w}_m^r)] E[g(\Phi_l^t + \omega_{l,k}^t \mid \mathbf{w}_m^t)]. \tag{17}$$

For a given cluster realization, we take the expectation over rays. To simplify the model, we assume that $\alpha_{l,k}$ of each ray follows a complex normal distribution $\mathrm{CN}(0, |\alpha_{l,0}|^2)$ with zero mean and a variance that is equal to the mean power decay of the first arrival ray within the lth cluster. Thus, we have

$$\frac{1}{K} \sum_{k=0}^{K-1} E(\alpha_{l,k} \alpha_{l,k}^*) = e^{-\Gamma_l/\Gamma}, \quad \text{for } l = 0, 1, \ldots, L-1. \tag{18}$$

Furthermore, according to (4), we assume that $\Gamma_l = l - 1/\Lambda \quad \text{for } l = 0, 1, \ldots, L-1$. Therefore, given a channel cluster realization, that is, the locations of clusters, the link gain is given by

$$\begin{aligned} G &= \frac{1}{LK} \sum_{l=0}^{L-1} E(\alpha_{l,k} \alpha_{l,k}^*) \int_0^{2\pi} f_\omega(\phi \mid \Phi_l^r) g(\phi \mid \mathbf{w}_m^r) d\phi \\ &\quad \times \int_0^{2\pi} f_\omega(\phi \mid \Phi_l^t) g(\phi \mid \mathbf{w}_m^t) d\phi \\ &= \frac{1}{L} [\, D(\Phi_0^r, \sigma, \mathbf{w}_m^r) \;\; \ldots \;\; D(\Phi_{L-1}^r, \sigma, \mathbf{w}_m^r) \,] \\ &\quad \times \mathrm{diag}\left[1 \;\; e^{-1/\Lambda\Gamma} \;\; \ldots \;\; e^{-(L-1)/\Lambda\Gamma} \right] \\ &\quad \times [\, D(\Phi_0^t, \sigma, \mathbf{w}_m^t) \;\; \ldots \;\; D(\Phi_{L-1}^t, \sigma, \mathbf{w}_m^t) \,]^T. \end{aligned} \tag{19}$$

The physical meanings of (19) are that, firstly, each route through a pair of Tx and Rx directional beam patterns pointing to a common cluster is associated with a mean power decay that increases exponentially with the cluster's delay time. Therefore, directional beam patterns should be steered towards early arrival clusters for a high-average link gain. Secondly, the mean link gain of the BF system decreases as the number of clusters increases. The channel is closer to a multipath-rich environment where the diversity scheme is more advantageous over the BF system. Finally, there exists extra diversity freedom by switching among different pairs of Tx and Rx beams to select different clusters as transmission routes in that the fading statistics of the rays within different clusters are assumed to be independent according to [11, 13]. The correlation between different routes is induced due to beam pattern overlapping.

Now we consider the case where there exist two clusters. For the simplicity of analysis, we arbitrarily set the positions of both clusters at both Tx and Rx sides as $\Phi_0^r = \Phi_0^t = 0^\circ$ and $\Phi_1^r = \Phi_1^t = 120^\circ$. By jointly pointing directional beam patterns towards 0° using $\mathbf{w}_1$ at both sides of the link, the link provides a joint gain of

$$G_1 = \frac{1}{2} \{ D(\Phi_0^r, \sigma, \mathbf{w}_1^r) D(\Phi_0^t, \sigma, \mathbf{w}_1^t) + e^{-1/\Lambda\Gamma} D(\Phi_1^r, \sigma, \mathbf{w}_1^r) D(\Phi_1^t, \sigma, \mathbf{w}_1^t) \}. \tag{20}$$

When both Tx and Rx point towards 120° using $\mathbf{w}_3$ the link gain is

$$G_2 = \frac{1}{2} \{ D(\Phi_0^r, \sigma, \mathbf{w}_3^r) D(\Phi_0^t, \sigma, \mathbf{w}_3^t) + e^{-1/\Lambda\Gamma} D(\Phi_1^r, \sigma, \mathbf{w}_3^r) D(\Phi_1^t, \sigma, \mathbf{w}_3^t) \}. \tag{21}$$

Therefore, the link gain difference between these two branches can be obtained as

$$\eta = \frac{D(\Phi_0^r, \sigma, \mathbf{w}_1^r) D(\Phi_0^t, \sigma, \mathbf{w}_1^t) + e^{-1/\Lambda\Gamma} D(\Phi_1^r, \sigma, \mathbf{w}_1^r) D(\Phi_1^t, \sigma, \mathbf{w}_1^t)}{D(\Phi_0^r, \sigma, \mathbf{w}_3^r) D(\Phi_0^t, \sigma, \mathbf{w}_3^t) + e^{-1/\Lambda\Gamma} D(\Phi_1^r, \sigma, \mathbf{w}_3^r) D(\Phi_1^t, \sigma, \mathbf{w}_3^t)}. \tag{22}$$

The weight vectors $\mathbf{w}_3^r$ and $\mathbf{w}_3^t$ produce directional beam patterns at both ends of the link towards 120°, whereas $\mathbf{w}_1^r$ and $\mathbf{w}_1^t$ produce directional beam pattern towards 0°. Therefore, $D(\Phi_0^r, \sigma | \mathbf{w}_3^r)$, $D(\Phi_0^t, \sigma | \mathbf{w}_3^t)$, $D(\Phi_1^r, \sigma | \mathbf{w}_1^r)$, and $D(\Phi_1^t, \sigma | \mathbf{w}_1^t)$ in (22) represent the DDGs when the beam patterns have a 120° misalignment. From Figure 7, we know that the DDG values with such misalignment are relatively small. Furthermore, we assume that the beam pattern for 0° and 120° are same. As stated in the previous section, we assume $\Gamma = 30$ nanoseconds, $1/\Lambda = 30$ nanosecond, $\sigma = 20^\circ$. Thus, (22) is simplified to

$$\eta \approx \frac{D(\Phi_0^r, \sigma, \mathbf{w}_1^r) D(\Phi_0^t, \sigma, \mathbf{w}_1^t)}{e^{-1/\Lambda\Gamma} D(\Phi_1^r, \sigma, \mathbf{w}_3^r) D(\Phi_1^t, \sigma, \mathbf{w}_3^t)} \approx e = 4.34\,\mathrm{dB}. \tag{23}$$

Therefore, by switching directional beam patterns jointly at both sides of the channel, we set up two wireless links with a 4.34 dB difference of link gains. We approximate the gain of each wireless link as

$$\begin{aligned} G_1 &\approx D(\Phi_0^r, \sigma, \mathbf{w}_1^r) D(\Phi_0^t, \sigma, \mathbf{w}_1^t), \\ G_2 &\approx e^{-1/\Lambda\Gamma} D(\Phi_1^r, \sigma, \mathbf{w}_3^r) D(\Phi_1^t, \sigma, \mathbf{w}_3^t). \end{aligned} \tag{24}$$

From Figure 7, we know that $G_1 = 2 \times 4.9 = 9.8$ dB and $G_2 = 5.5$ dB for the channel with $\sigma = 20^\circ$. Please note that the link gain calculated in our model is normalized such that when omnidirectional antennas are installed at both ends of the link, the link gain G is 0 dB.

3.3. Channel correlation

As explained previously, by jointly switching different Tx and Rx beam patterns, the two wireless links can be exploited to

achieve certain diversity advantage. The correlation between the two wireless links is induced due to beam pattern overlapping. In this subsection, we examine the beam pattern correlation.

We assume that there are two clusters in the clustering DDRC as shown in Figure 5. Furthermore, each cluster's center is assumed to be aligned with the direction of a beam pattern. Therefore, there is no beam pattern direction misalignment. Given the distribution of rays $f_\omega(\phi|\Phi_1,\Phi_2)$ in (14), the correlation for the two directional beam patterns $g(\phi|\mathbf{w}_m)$ and $g(\phi|\mathbf{w}_n)$ can be expressed as

$$\rho_{m,n} = \frac{\left|\int_0^{2\pi} f_\omega(\phi|\Phi_1,\Phi_2)\mathbf{w}_m^T\boldsymbol{\alpha}(\phi)\boldsymbol{\alpha}^H(\phi)\mathbf{w}_n^* d\phi\right|}{\sqrt{\int_0^{2\pi} f_\omega(\phi|\Phi_1,\Phi_2)g(\phi|\mathbf{w}_m)d\phi}} \times \frac{\left|\int_0^{2\pi} f_\omega(\phi|\Phi_1,\Phi_2)\mathbf{w}_m^T\boldsymbol{\alpha}(\phi)\boldsymbol{\alpha}^H(\phi)\mathbf{w}_n^* d\phi\right|}{\sqrt{\int_0^{2\pi} f_\omega(\phi|\Phi_1,\Phi_2)g(\phi|\mathbf{w}_n)d\phi}}, \tag{25}$$

where $f(\phi)$ is given in (14). The correlation $\rho_{m,n}$ is shown in Figure 8 for different values of σ. The markers in the figure indicate the correlation for six discrete beam patterns, whereas the dashed lines show the correlation for continuously rotated beam patterns. We notice that the correlation decreases as the angular spread of rays increases. The back lobe of the beam patterns as shown in Figure 4 induces the high correlation for two beam patterns pointing the opposite directions (180° angular separation).

Knowing the correlation of any given two beam patterns at each side of the wireless link, the complex correlation of two link channels constructed by jointly pointing directional beam patterns towards the same clusters is given as $\rho = \rho^r_{m,n}\rho^t_{m,n}$. For the channel realization with $\sigma = 20°$, $\Phi^r_0 = \Phi^t_0 = 0°$, and $\Phi^r_1 = \Phi^t_1 = 120°$, we obtain the channel correlation as $\rho = 0.8 \times 0.8 = 0.64$.

Using the DDG and beam pattern correlation, we set up an analytical model of the BF system. In the following section, we examine the channel capacity of the BF system based on this analytical model.

4. NUMERICAL RESULT

In Section 3, we have obtained the link gains and the correlation of two wireless links. In this section, we examine the link performance of the BF system and compare it with a MIMO system. To simplify the performance evaluation process and make the system independent of particular modulation schemes and coding techniques, we use the Shannon's theoretical channel capacity and the outage rate to evaluate the link performance and investigate the benefits from beam pattern diversity gain.

4.1. Outage probability relative to output SNR

In the case of two clusters, after the Tx and Rx have identified the clusters, two link channels can be established by jointly directing beam patterns at both Tx and Rx sides towards the common cluster. Switching between these two channels provides a diversity gain. In this paper, we denote the link from Tx to Rx through the cluster at $\Phi^r_0 = \Phi^t_0 = 0°$ as channel no.1, and denote that through the cluster at $\Phi^r_1 = \Phi^t_1 = 120°$ as channel no.2. In the previous subsections, we have calculated that their complex envelop correlation is 0.8×0.8, and the difference of link gains is 4.34 dB. Without selection combining (SC), each link experiences a Rayleigh fading process. The outage rate of the output SNR relative to the input SNR at each channel is given by

$$\Pr(r < x) = F_r(x) = 1 - \exp\left(-\frac{x}{G_1}\right), \quad \text{for } i = 1, \text{ or } 2, \tag{26}$$

where r is the instantaneous link gain.

The outage rate with the SC of these two channels is obtained by calculating

$$\Pr(r < x) = F_r(x) = 1 - \exp\left(-\frac{x}{G_1}\right)Q(b, a|\rho|) - \exp\left(-\frac{x}{G_2}\right)(1 - Q(b|\rho|, a)). \tag{27}$$

$Q(a,b)$ is the Marcum's Q-function:

$$Q(a,b) = \int_b^\infty \exp\{-1/2(a^2+x^2)\}I_0(ax)x\,dx, \tag{28}$$

and I_0 is the modified Bessel function:

$$a = \sqrt{\frac{2x}{G_1(1-|\rho|^2)}}, \quad b = \sqrt{\frac{2x}{G_2(1-|\rho|^2)}}. \tag{29}$$

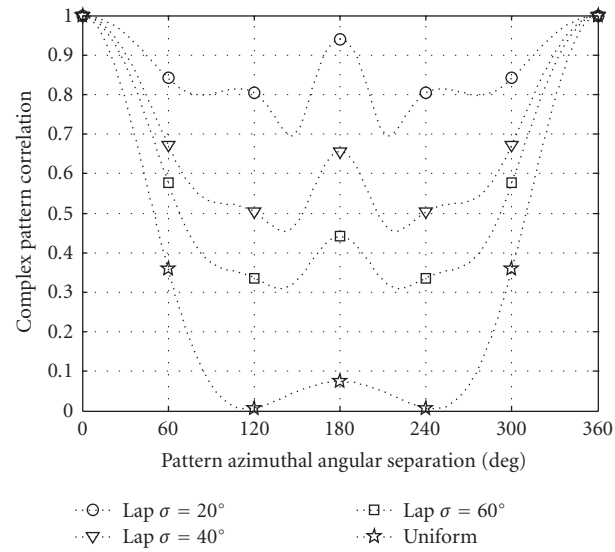

FIGURE 8: Complex correlation of beam patterns in the presence of a given angular distribution property of the channel.

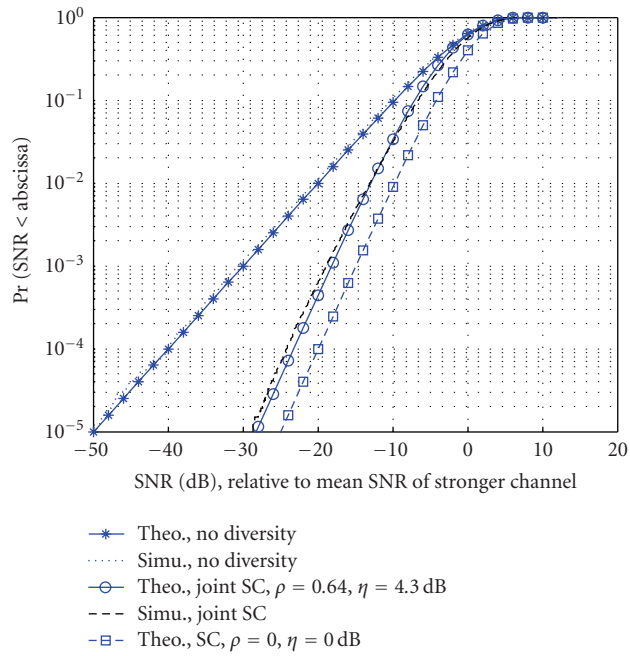

Figure 9: The outage rates of different channels using directional antennas at both ends of the wireless links.

The outage rates of relative output SNR from the channels without and with SC technique are shown in Figure 9, respectively. Given the DDGs for the two channels and their correlation in the presence of two wave clusters, we calculate the theoretical outage rate with the SC of two channels using (26) and (27). The curve without a diversity approach shows the typical Rayleigh fading. The curve with the square markers shows the situation when ideal SC of two channels with equal SNRs and independent fading processes is employed. Compared to the curve without diversity, we can see that even the two channels have a 4.3 dB difference of link gains and a correlation of $\rho = 0.64$, significant diversity gain is still achieved by jointly switching between different pairs of Tx and Rx directional beam patterns.

Simulation is also carried out for the same channel realization. Totally, 1000 ray realizations are created. In addition, for each ray realization, 1000 fading channels are randomly generated. At each instant channel realization, the Tx and Rx ESPAR antennas jointly switch to a common cluster that gives the maximum instantaneous link gain. The output link gain after SC is used to compute the outage rate. The simulation results match closely with the theoretical results and show significant performance. This verifies our analytical model. In the following analysis, we will use this analytical model to examine the performance of the BF system and compare it with a MIMO system.

Please note that the difference between the theoretical and simulated results is due to (a) the simplification of distribution of amplitude of rays within each cluster as a normal distribution with the variance equal to the mean power decay of the first arrival ray in (18): (b) the approximation of the difference between the link gains of two channels in (23).

4.2. Channel capacity

Given an instantaneous link gain r and the average SNR, the channel capacity of the BF system is given by

$$C_{\mathrm{BF}} = \log(1 + r\mathrm{SNR}). \tag{30}$$

Using the outage probabilities for the BF system without and with diversity given in (26) and (27), respectively, we obtain the outage probably of C_{BF} as

$$\begin{aligned}\Pr(C_{\mathrm{BF}} < C_{\mathrm{out}}) = F_{\mathrm{BF}}(C_{\mathrm{out}}) &= \Pr\left(r < \frac{2^{C_{\mathrm{out}}} - 1}{\mathrm{SNR}}\right) \\ &= F_r\left(\frac{2^{C_{\mathrm{out}}} - 1}{\mathrm{SNR}}\right).\end{aligned} \tag{31}$$

In order to compare the performance of the BF system with that of a MIMO system, we also numerically obtain the channel capacity of a MIMO system that is set up with linear antenna arrays of half-wavelength interelement spacing at both ends of the wireless link. The MIMO channel capacity is dependent on the array orientation with respect to the position of wave clusters [21]. To compare the BF system and the MIMO system at a given cluster realization, we assume that at each side of the link, the directions of the two clusters with respect to the end-fire direction of the linear array are 0° and 120°, respectively. All the elements of the linear arrays have the same omnidirectional beam pattern. Thus, the DDG of each element is 0 dB. The steering vector of the linear array that consists of M array elements reads

$$\boldsymbol{\alpha}(\phi) = \left[\begin{array}{cccc} 1 & e^{-j\pi\cos(\phi)} & \ldots & e^{-j\pi(M-1)\cos(\phi)} \end{array}\right]^T. \tag{32}$$

We employ Wallace's method [11] to obtain the MIMO channel model in a clustering DDRC. In the following analysis, we refer to this MIMO channel model as Wallace's MIMO model. Given the SRC of a clustering DDRC in (1), the spatial channel model for the MIMO system in the clustering DDRC is given by

$$\mathbf{H} = \boldsymbol{\alpha}(\phi^r) * h(\phi^r, \phi^t) * \boldsymbol{\alpha}^T(\phi^t), \tag{33}$$

with each matrix entry being normalized as $E[|\mathbf{H}(i,j)|^2] = 1$. In this study, we assume that the linear arrays at both ends of the link have two elements, that is, $M = 2$. For the MIMO system in an ideal statistical model [7], the entries of $\mathbf{H}$ are given as independent and identically distributed (iid) complex Gaussian random variables (RV), that is, $\mathbf{H}(i,j) \sim \mathrm{CN}(0,1)$. We here after refer to this MIMO channel model as Foschini's MIMO channel. The channel capacity of a 2×2 MIMO system is given by

$$C_{\mathrm{MIMO}} = \log_2 \det\left(\mathbf{I} + \frac{\mathrm{SNR}}{2}\mathbf{H}\mathbf{H}^H\right), \tag{34}$$

where superscript $(\cdot)^H$ denotes conjugate transpose, and $\mathbf{I}$ is an identity matrix. Furthermore, $\det(\cdot)$ denotes matrix determinant.

The channel capacities for both BF and MIMO systems when SNR = 10 dB are shown in Figure 10. The line "omni-omni, gain = 0 dB" refers to the situation when one omnidirectional antenna (DDG is 0 dB) is installed at each side of

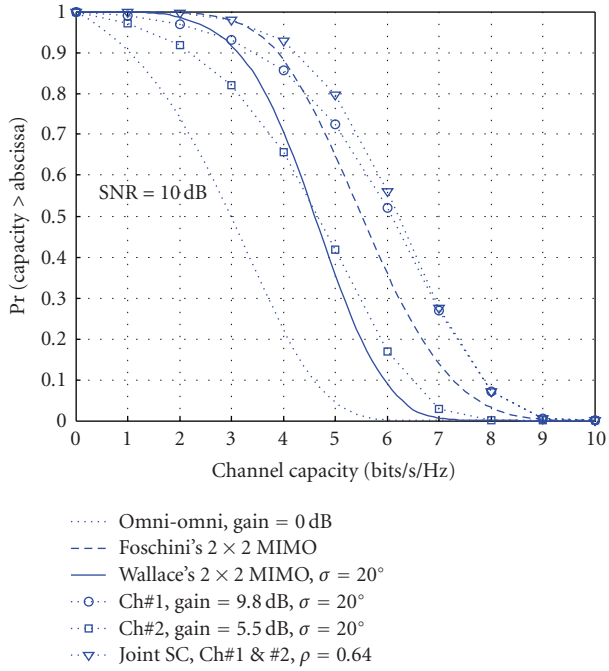

Figure 10: Shannon's theoretical channel capacities of both BF and MIMO systems in different scenarios.

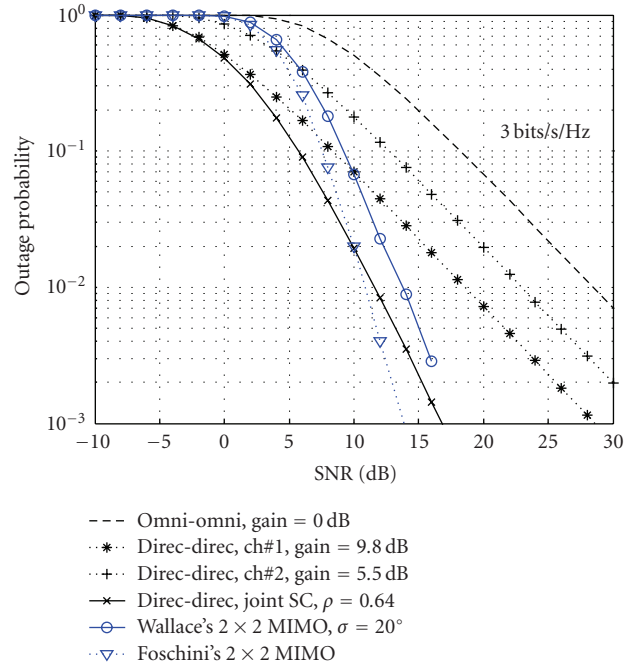

Figure 11: Outage rates of channel capacity at 3 bits/sec/Hz for both BF and MIMO systems in different scenarios.

the link. The dashed line shows the theoretical channel capacity of the Foschini's 2×2 MIMO system as in [7]. This channel capacity is predicted based on the assumption of rich multipath. The solid line in Figure 10 shows the channel capacity of the Wallace's 2×2 MIMO system in a clustering DDRC model [11]. As expected, in a clustering channel, the channel capacity of a MIMO system is lower than that predicted in ideal statistical model.

When directional beam patterns are jointly employed towards the first arrival cluster, the Tx and Rx directional antennas jointly provide a DDG of $G_1 = 9.8$ dB to the wireless channel, which significantly increases the channel capacity. It is interesting to note that the ergodic capacity achieved by the BF system is even higher than that of the Foschini's 2×2 MIMO channel [7]. As shown in Figure 10, SC of these two links channels does not provide significant gain in terms of ergodic capacity. This is consistent with the conclusion in [22] that the influence of the diversity gain on the ergodic channel capacity is negligible. However, as will be shown in the following analysis, the diversity advantage of SC does significantly reduce the outage probability, thus improving the stability of wireless transmission.

Figure 11 shows the outage rate for $C_{\text{out}} = 3$ bits/sec/Hz at different SNR situations. Compared with the curve of a scalar Rayleigh fading channel "omni-omni, gain = 0 dB," that is, one onmidirectional antenna is installed at each end of the wireless link, the outage curves for both channel #1 and channel #2 are moved to the left by the joint DDG. This is due to the fact that the DDG obtained from using directional antennas directly increase the average SNR of the wireless link. When SC of the two channels is employed, the outage probability is further reduced by the diversity gain. Thus, the required SNR to achieve the same outage rate at a given channel capacity is significantly reduced.

In the same figure, the outage probabilities at $C_{\text{out}} = 3$ bits/s/Hz of the 2×2 MIMO system in both ideal statistical channel and clustering DDRC are also plotted. It is interesting to note that in a low-SNR environment, the BF system with SC outperforms the Wallace's MIMO system in terms of the outage probability. This shows that in a low-SNR environment, the BF system provides a better wireless link in terms of stability than that of a MIMO system in the same clustering environment.

5. CONCLUSION AND DISCUSSION

In this paper, we proposed a BF system that directs both Tx and Rx directional beam patterns towards a common wave cluster. In a clustering DDRC, we obtained the DDG and beam pattern correlation for the BF system. Based on these results, we built an analytical model through which the channel capacity of the BF system was obtained. The close match between the simulation and analytical results justifies our model. Using the outage probability of the theoretical channel capacity, we have shown that the DDG of the BF directly increases the mean SNR of the wireless link, thus achieving a direct increase of the ergodic channel capacity. By jointly switching between different pairs of Tx and Rx directional beam patterns towards different wave clusters, the system also provides diversity gain to combat against multipath fading, thus reducing the outage probability of the channel capacity.

By comparing the proposed BF system with a MIMO system, we have shown that for a given cluster realization in a

clustering DDRC, the BF system provides a higher-ergodic channel capacity. This is because of the significant DDG that is achieved by employing directional antennas in a clustering channel. Furthermore, in a low-SNR environment, the BF system that employs SC outperforms the MIMO system in terms of outage probability of the channel capacity. Thus, the BF system provides a wireless link that is of higher stability than that of the MIMO system.

From the viewpoint of practical implementations of adaptive antennas, if the beamforming network (BFN) is implemented at the RF stage, we can employ a directional antenna at a transceiver that has only one RF channel. This simplifies the system structure and reduces the DC power consumption. As an implementation example, the ESPAR antennas are employed in this study. The MIMO systems, on the other hand, require independent RF channels, increasing system complexity and cost. Since performance gains similar to MIMO can be obtained with the less expensive BF system for realistic environments with cluster-type scattering, the results suggest that BF is a good candidate for advanced indoor wireless communications networks.

REFERENCES

[1] K. Sheikh, D. Gesbert, D. Gore, and A. Paulraj, "Smart antennas for broadband wireless access networks," *IEEE Communications Magazine*, vol. 37, no. 11, pp. 100–105, 1999.

[2] J. Litva and T. K.-Y. Lo, *Digital Beamforming in Wireless Communications*, Artech House, Boston, Mass, USA, 1996.

[3] C. Sun and N. C. Karmakar, "Adaptive array antennas," in *Encyclopedia of RF and Microwave Engineering*, K. Chang, Ed., p. 5832, John Wiley & Sons, New York, NY, USA, 2005.

[4] C. Passerini, M. Missiroli, G. Riva, and M. Frullone, "Adaptive antenna arrays for reducing the delay spread in indoor radio channels," *Electronics Letters*, vol. 32, no. 4, pp. 280–281, 1996.

[5] D. G. Brennan, "Linear diversity combining techniques," *Proceedings of the IEEE*, vol. 91, no. 2, pp. 331–356, 2003.

[6] M. Schwartz, W. R. Bennett, and S. Stein, *Communication Systems and Techniques*, McGraw-Hill, New York, NY, USA, 1966.

[7] G. J. Foschini and M. J. Gans, "On limits of wireless communications in a fading environment when using multiple antennas," *Wireless Personal Communications*, vol. 6, no. 3, pp. 311–335, 1998.

[8] A. F. Naguib, N. Seshádri, and A. R. Calderbank, "Increasing data rate over wireless channels," *IEEE Signal Processing Magazine*, vol. 17, no. 3, pp. 76–92, 2000.

[9] M. Steinbauer, A. F. Molisch, and E. Bonek, "The double-directional radio channel," *IEEE Antennas & Propagation Magazine*, vol. 43, no. 4, pp. 51–63, 2001.

[10] C. Sun and N. C. Karmakar, "Direction of arrival estimation with a novel single-port smart antenna," *EURASIP Journal on Applied Signal Processing*, vol. 2004, no. 9, pp. 1364–1375, 2004.

[11] J. W. Wallace and M. A. Jensen, "Modeling the indoor MIMO wireless channel," *IEEE Transactions on Antennas and Propagation*, vol. 50, no. 5, pp. 591–599, 2002.

[12] A. Saleh and R. Valenzuela, "A statistical model for indoor multipath propagation," *IEEE Journal on Selected Areas in Communications*, vol. 5, no. 2, pp. 128–137, 1987.

[13] Q. H. Spencer, B. D. Jeffs, M. A. Jensen, and A. L. Swindlehurst, "Modeling the statistical time and angle of arrival characteristics of an indoor multipath channel," *IEEE Journal on Selected Areas in Communications*, vol. 18, no. 3, pp. 347–360, 2000.

[14] M. A. Jensen and J. W. Wallace, "A review of antennas and propagation for MIMO wireless communications," *IEEE Transactions on Antennas and Propagation*, vol. 52, no. 11, pp. 2810–2824, 2004.

[15] T. Ohira and J. Cheng, "Analog smart antennas," in *Adaptive Antenna Arrays: Trends and Applications*, S. Chandran, Ed., pp. 184–204, Springer, New York, NY, USA, 2004.

[16] C. Sun, A. Hirata, T. Ohira, and N. C. Karmakar, "Fast beamforming of electronically steerable parasitic array radiator antennas: theory and experiment," *IEEE Transactions on Antennas and Propagation*, vol. 52, no. 7, pp. 1819–1832, 2004.

[17] H. Kawakami and T. Ohira, "Electrically steerable passive array radiator (ESPAR) antennas," *IEEE Antennas & Propagation Magazine*, vol. 47, no. 2, pp. 43–50, 2005.

[18] http://www.qsl.net/wb6tpu/swindex.html.

[19] C.-C. Chong, C.-M. Tan, D. I. Laurenson, S. McLaughlin, M. A. Beach, and A. R. Nix, "A new statistical wideband spatio-temporal channel model for 5-GHz band WLAN systems," *IEEE Journal on Selected Areas in Communications*, vol. 21, no. 2, pp. 139–150, 2003.

[20] R. Vaugh and J. B. Andersen, *Channels, Propagation and Antennas for Mobile Communications*, IEE Electromagnetic Waves Series, Institution of Electrical Engineers, Glasgow, UK, 2003.

[21] X. Li and Z.-P. Nie, "Effect of array orientation on performance of MIMO wireless channels," *IEEE Antennas and Wireless Propagation Letters*, vol. 3, no. 1, pp. 368–371, 2004.

[22] C. G. Günther, "Comment on "estimate of channel capacity in Rayleigh fading environment"" *IEEE Transactions on Vehicular Technology*, vol. 45, no. 2, pp. 401–403, 1996.